Supporting Information for

Achieving Multifunction MOFs/polymer Quasi-Solid Electrolytes by Functional Molecule Encapsulation in MOFs

Xu Li[a,b]*, Hongwei Pan*[b]*, Guijie Yin* [a,b]*, Yang Xiang*[a,b]*, Xitao Lin*[a]*, Zhu Liu*[b]*, Yinzhu Jiang*[b,c]*, Qun Hui*[a]**, Xuan Zhang*[b,c]**, Maowen Xu*[a]***

[a] Chongqing Key Laboratory of Battery Materials and Technologies, School of Materials and Energy, Southwest University, Chongqing 400715, P. R. China.

[b] Hangzhou Global Scientific and Technological Innovation Center (HIC), Zhejiang University, Hangzhou 310027, China.

[c] School of Materials Science and Engineering, State Key Laboratory of Clean Energy Utilization, Zhejiang University, Hangzhou 310027, China.

* Corresponding author. Email: xumaowen@swu.edu.cn; xuanzhangzju@zju.edu.cn;
qhui01@swu.edu.cn.

Experimental section

Materials

The chemicals used in this work are listed as follows: Zirconium (IV) chloride $ZrCl_4$ (99%), Terephthalic acid (99%), Polyvinylidene fluoride (PVDF), hexachlorocyclotriphosphazene (HCCP, 98%), N-N dimethylformamide (DMF), bis (trifluoromethanesulfony) imide (LiTFSI) were purchased from Aladdin. Methanol (AR) and N-methyl pyrrolidone (NMP) were purchased from Sinopharm Chemical Reagent Co., Ltd. Poly (vinylidene fluoride-co-hexafluoropropylene) (PVDF-HFP) was obtained from Sigma-Aldrich. $LiFePO_4$ (LFP) and acetylene black (AB) were purchased from Kejing Star Technology Co., Ltd., Shenzhen, China. Electrolyte (1 M $LiPF_6$) in ethylene carbonate (EC)/dimethyl carbonate (DMC)/ethyl methyl carbonate (EMC) (1:1:1, v/v) without additive was provided by Dodo Chem.

Materials preparation

Synthesis of UiO-66 / HCCP-50@UiO-66 / HCCP-100@UiO-66

375 mg zirconium chloride ($ZrCl_4$) was added to a mixed solution of 15 mL N, N-dimethylformamide (DMF) and 3 mL hydrochloric acid (HCl, 37wt%), and the suspension was sonicated until $ZrCl_4$ was completely dissolved. Then, 369 mg of terephthalic acid (TPA), 100 mg of HCCP and 30 mL of DMF were added to the above solution, and the same ultrasonic treatment was performed until the solid was completely dissolved. Finally, the mixed solution was transferred to a Teflon-lined autoclave, and the hydrothermal reaction was carried out in an oven at 80°C for 12 hours. Then, the solution in the Teflon-lined autoclave was taken out, centrifuged, and washed three times with DMF and ethanol. The resulting white powder was named **HCCP-100@UiO-66** or **HCCP@UiO-66**. The synthesis method of **UiO-66** and **HCCP-50@UiO-66** is the same as the above method, except that HCCP is not added or 50 mg HCCP is added.

Synthesis of different QSSEs

1 g PVDF-HFP and 0.5 g LiTFSI were dispersed in 5 mL of 1-methyl-2-pyrrolidone (NMP, 99.5%) and stirred at 60 °C for 6 hours to form a uniform mixture. Spread the mixture flat on an aluminum foil using a 250 μm scraper and dry under vacuum at 60 °C. Place the dry membrane off the aluminum foil to obtain PVDF-HFP membrane, named **P-QSSE**. The production method for QSSEs is identical to the previously mentioned method,but the difference lies in the filler material. **PHU-QSSE** consists of PVDF-HFP, LiTFSI and 0.5g HCCP@UiO-66.**PU-QSSE** is composed of PVDF-HFP, LiTFSI and UiO-66. **PH-QSSE** consists of PVDF-HFP, LiTFSI and HCCP.

Electrolyte and electrode preparation

The prepared QSSEs were cut into 16 mm diameter discs and placed in a glove box filled with argon atmosphere. Commercial $LiFePO_4$, AB and PVDF were mixed in NMP with a mass ratio of 7: 2: 1 to obtain the cathode. The loading of cathode material on aluminum foil is not less than 2 mg/cm^2. Long cycle, rate cycle and other tests of batteries carry out on the LAND Battery Test System. EIS, the ionic conductivity and Li^+ transfer number were tested by the CHI660E electrochemical workstation.

Samples characterization

The ZEISS Sigma 300 (ZEISS, Germany) was used to obtain the morphology and elemental distribution of UiO-66 and HCCP@UiO-66. QSSEs was observed by FESEM (JEOL JSM-7800F). Powder samples and QSSEs were tested by (XRD, Bruker, Advance D8A A25). X-ray photoelectron spectroscopy (XPS，Escalab 250XI，Thermo Scientific) was used to tested the P and Cl elementals of HCCP@UIO-66. Thermogravimetric analysis (TGA, Q50, USA) characterization of powder samples and QSSEs was carried out. The characteristic of specific surface area and pore size distribution of UiO-66, HCCP-50@UiO-66, and HCCP-100@UiO-66 were analyzed by the BET Instrument (Quadrasorb EVO 2QDSMP30, Quantachrome, USA). The P content of HCCP-100@UiO-66 was utilized by Inductively coupled plasma mass spectrometry (ICP-MS, Elan DRCII, Perkin-Elmer Sciex). A JASCO microscope spectrometer (NRS-1000DT) was used to test Raman spectra of QSSEs and powder samples. The FT-IR spectra of QSSEs was performed by a Thermo Scientific Nicolet iS20. Using FTT FAA-PCFC

(FTT, England) to test Micro-combustion calorimeter (MCC) data of P-QSSE,PU-QSSE and PHU-QSSE.

The thermal shrinkage measurement

The thermal shrinkages of QSSEs and Celgard 2400 were conducted by heating the QSSEs and Celgard 2400 for 20 min at a temperature of 180 °C.

$$S(\%) = \frac{D_a - D_b}{D_b} \times 100\% \tag{1}$$

where D_a and D_b are the diameters of the QSSEs and Celgard 2400 before and after heating.

Electrochemical measurements

CR2025 coin cells were assembled with LFP cathode, electrolyte (1M $LiPF_6$ in EC/DMC/EMC with a volume ratio of 1:1:1) and the prepared separator. By means of a battery testing system (LAND, China). A minimal amount of LEs (<10 μL) should be infiltrated onto the surface to wet the interface when assembling cells with QSSEs.

Ionic conductivity of the QSSE was tested by stainless|QSSEs|stainless batteries with a frequency range of 0.1 Hz to 1 kHz using the CHI660E electrochemical workstation.

$$\sigma = \frac{L}{R \times A} \tag{2}$$

where $\sigma(S \cdot cm^{-2})$, $L(cm)$, $R(\Omega)$ and $A(cm^2)$ stand for the ionic conductivity, QSSE thickness, bulk resistance and surface area of the electrode, respectively.

The Li^+ transfer number was tested by equation (3):

$$t_{Li^+} = \frac{I_s(\triangle V - I_0R_0)}{I_0(\triangle V - I_sR_s)} \tag{3}$$

$\triangle V(10\,mV)$ represents the polarization voltage. I_0 and I_s represent the initial current and the steady current. R_0 and R_s represent the initial resistance and the steady resistance.

The activation energy (E_a) was calculated based on the Arrhenius equation (4):

$$\sigma(T) = AT^{-1}e^{-E_a/RT} \tag{4}$$

A ,e,R,T and E_a represent the characteristic constant of the given reaction, the natural logarithm (2.718), the gas constant (8.314 J mol^{-1} K^{-1}) ， the thermodynamic temperature and the activation energy (kJ mol^{-1})， respectively.

To test the cyclic stability of PHU-QSSE, the cyclic voltammetry (CV) test of the LFP||Li cell was performed within a voltage range of 2.4-4.1 V with a scan rate of 1 mV using a CHI660E.

Electrochemical impedance spectroscopy (EIS) measurements were conducted using an electrochemical analyzer to ascertain the AC impedance. The procedure for the test is outlined below: The components were stacked in the sequence of anode /composite solid-state electrolytes (QSSEs)/LFP cathode. Post-assembly, the cell was removed and allowed to rest for a duration of 12 hours. Subsequently, the EIS feature of the electrochemical analyzer was utilized for evaluation over a frequency spectrum spanning from 10 mHz to 100 kHz.

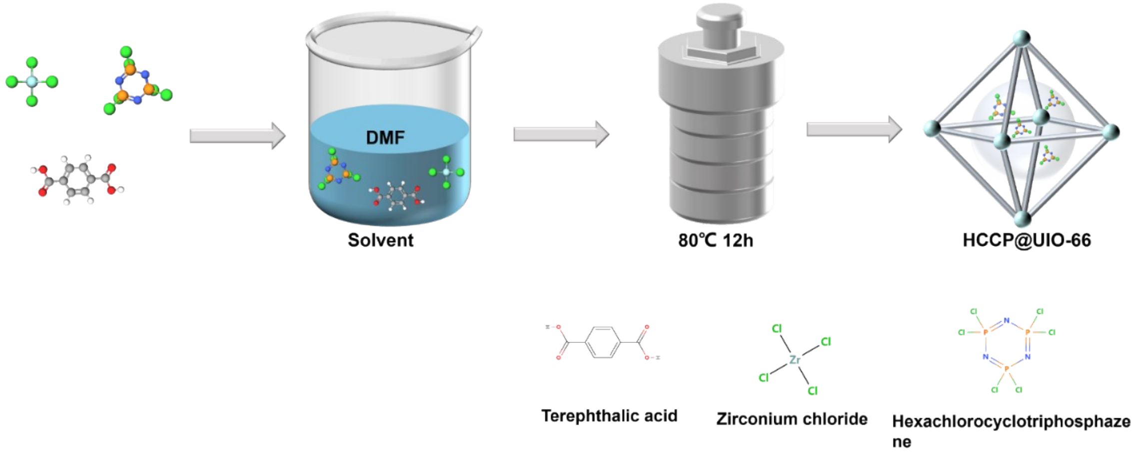

Fig. S1 Schematic diagram of the one-pot synthesis of HCCP@UiO-66.

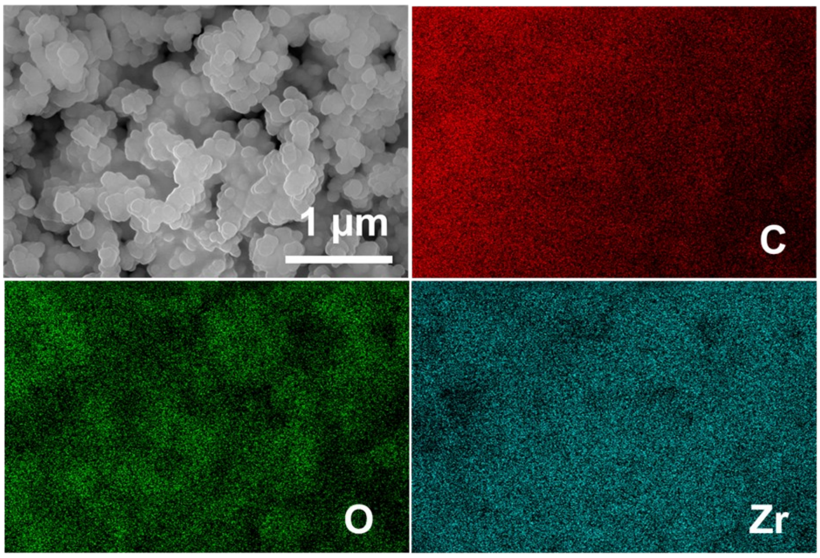

Fig. S2 SEM images of the UiO-66 and EDS mapping of elements C, O and Zr.

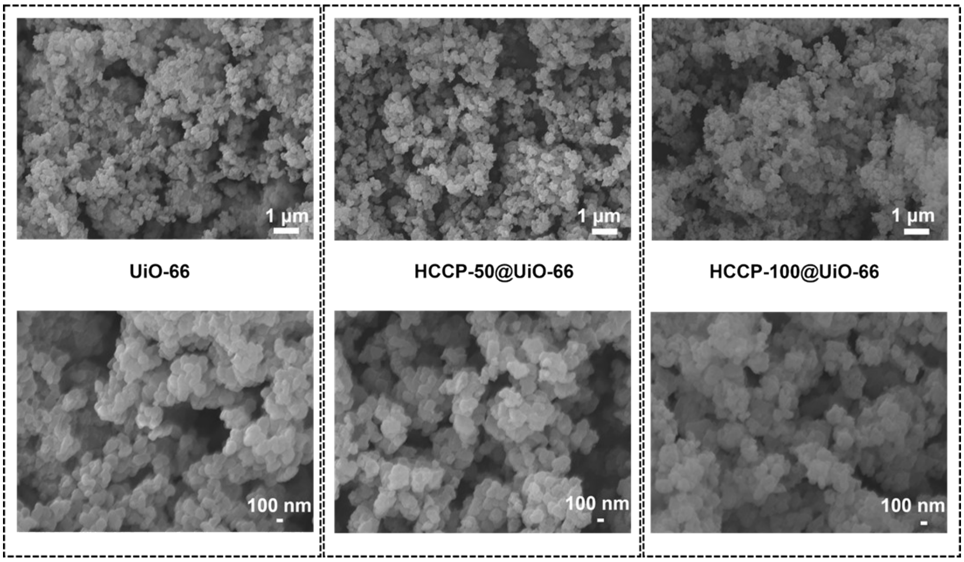

Fig. S3 The SEM images of UiO-66, HCCP-50@UiO-66 and HCCP-100@UiO-66.

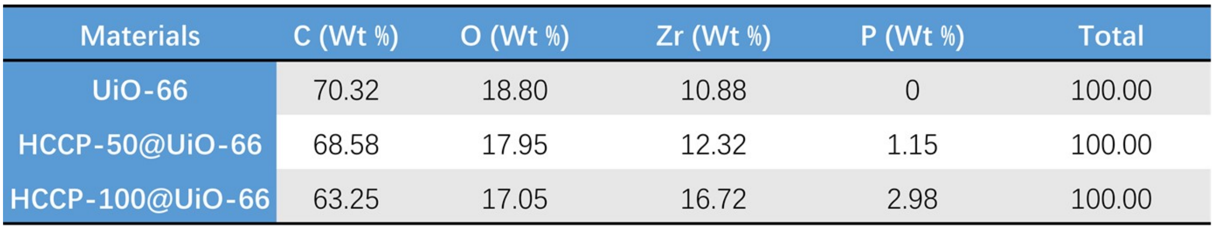

Materials	C (Wt %)	O (Wt %)	Zr (Wt %)	P (Wt %)	Total
UiO-66	70.32	18.80	10.88	0	100.00
HCCP-50@UiO-66	68.58	17.95	12.32	1.15	100.00
HCCP-100@UiO-66	63.25	17.05	16.72	2.98	100.00

Fig. S4 The elements content of EDS mapping of different samples.

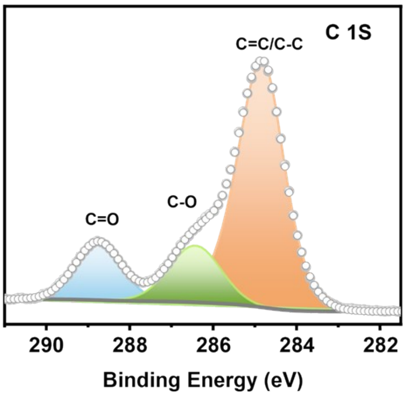

Fig. S5 XPS spectra of C 1S in HCCP@UiO-66.

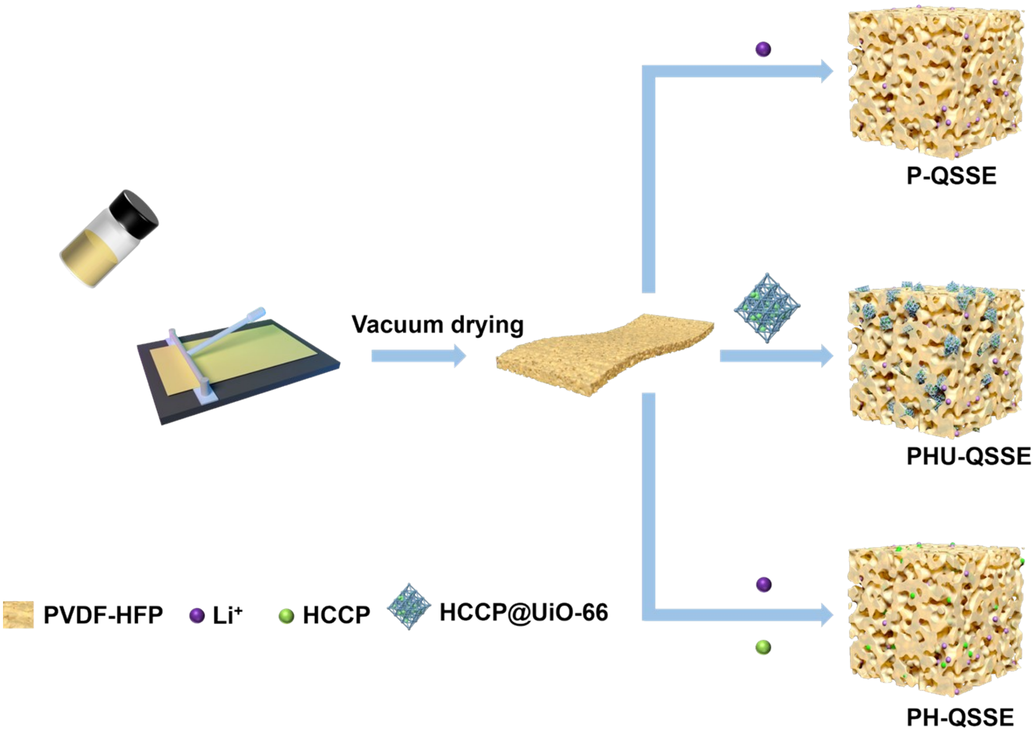

Fig. S6 The process to produce QSSEs.

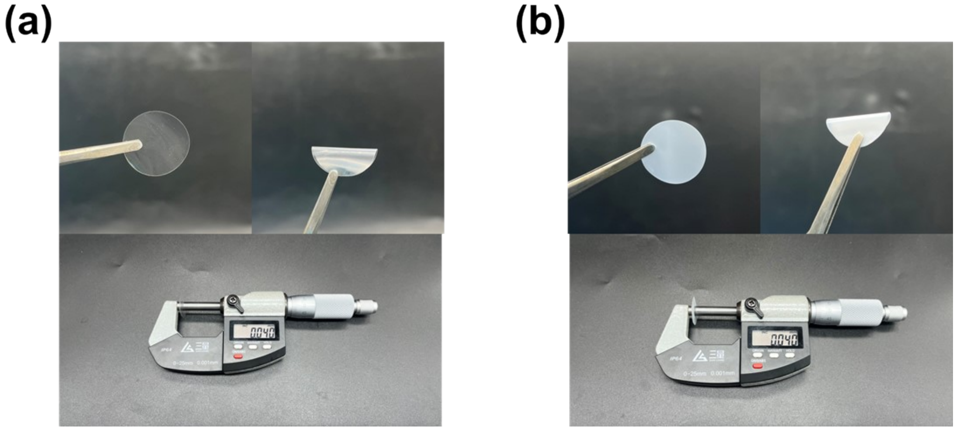

Fig. S7 (a) Optical photographs of P-QSSE and (b) PU-QSSE.

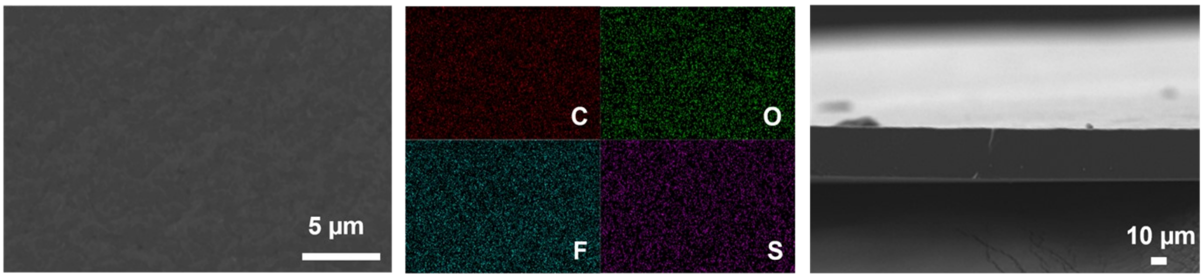

Fig. S8 SEM images of the P-QSSE surface, the EDS mapping of C, O, F and S elementals and the SEM image of P-QSSE cross-section.

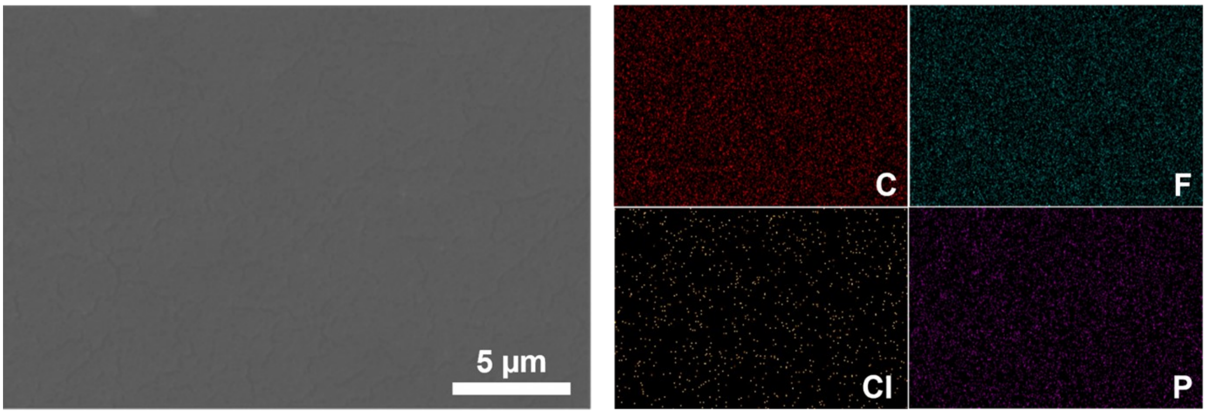

Fig. S9 (d) SEM images of the PH-QSSE surface and (e) the EDS mapping of C, Cl, F and P elementals.

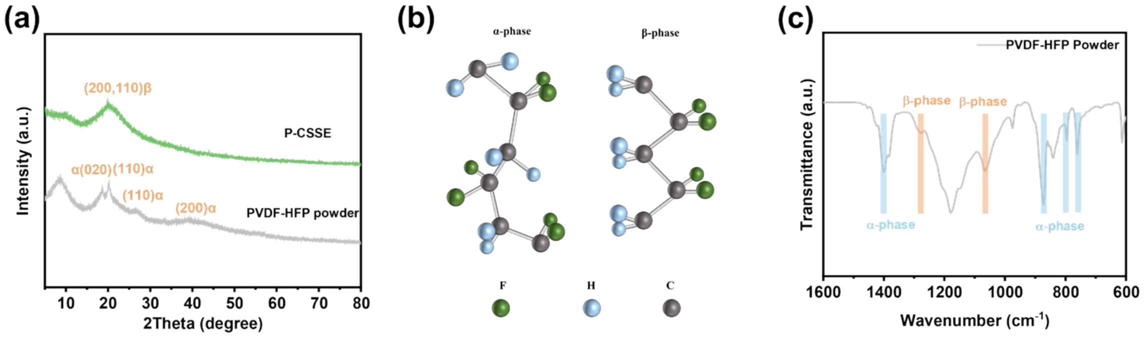

Fig. S10 (a) XRD patterns of PVDF-HFP powder and P-QSSE. (b) α and β phase of PVDF-HFP powder. (c) FT-IR spectra of PVDF-HFP powder.

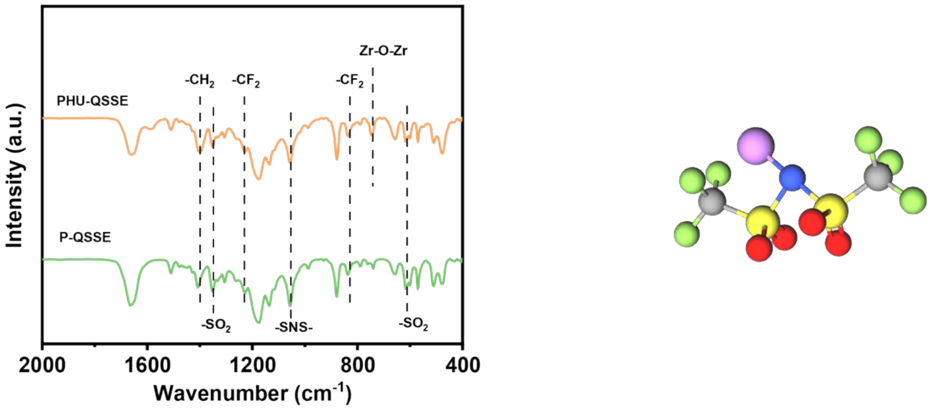

Fig. S11 FT-IR spectra of P-QSSE and PHU-QSSE. Ball-and-stick modelling of LiTFSI.

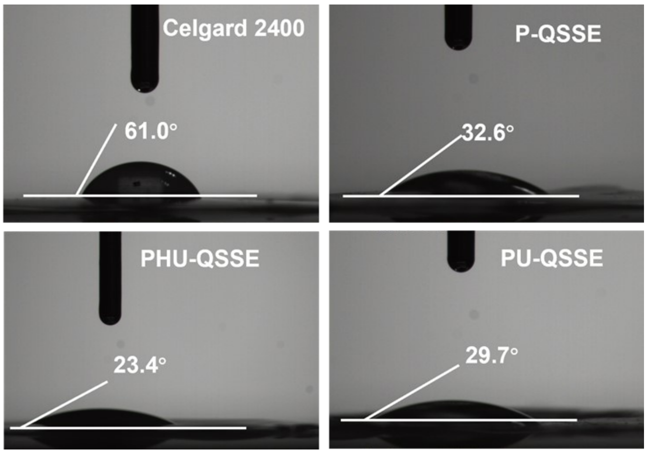

Fig. S12 The affinity between different membranes and LEs is measured by contact angle. The contact angle follows the order (Celgard 2400 (61.0°)＞P-QSSE (32.6°) > PU-QSSE (29.7°) > PHU-QSSE (23.4°)).

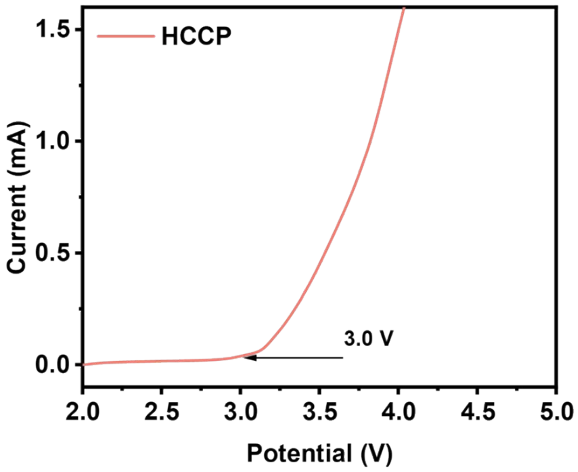

Fig. S13 Decomposition voltage of HCCP.

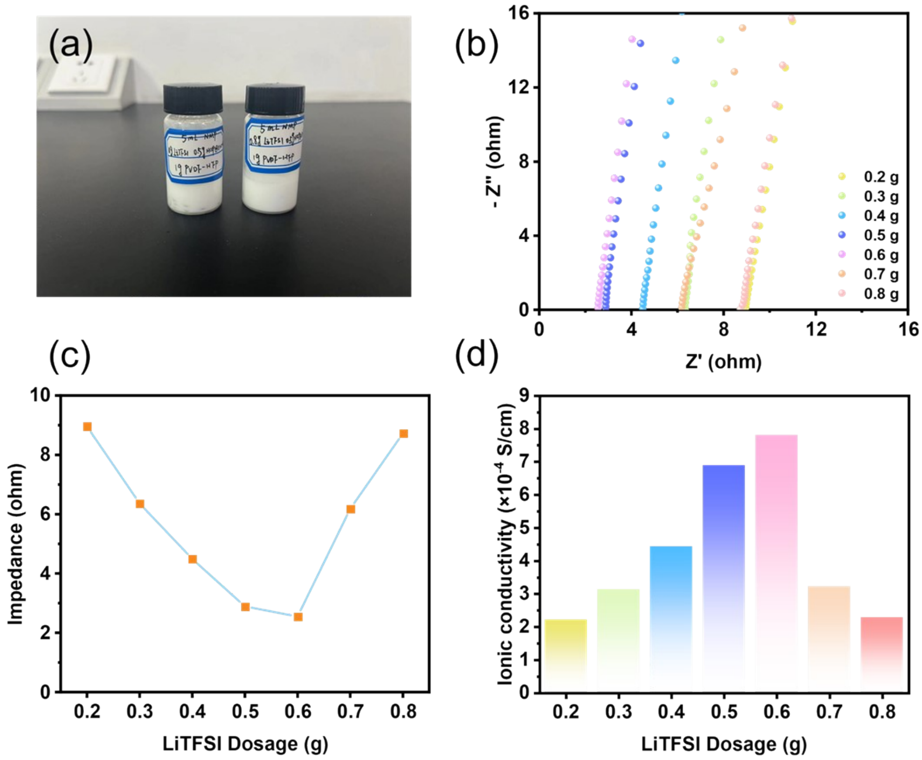

Fig. S14 (a) Preparation of electrolyte with high lithium content. (b,c) AC impedance of electrolytes with different lithium salt contents. (d) Ionic conductivity of electrolytes with different lithium salt dosages.

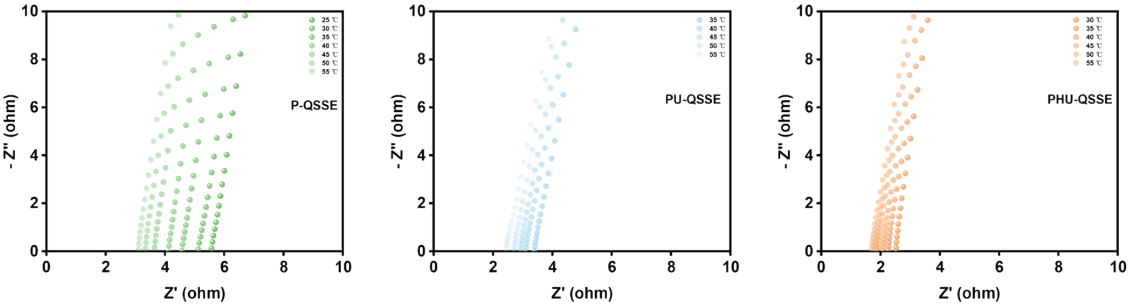

Fig. S15 Variable-temperature ionic conductivity of different QSSEs.

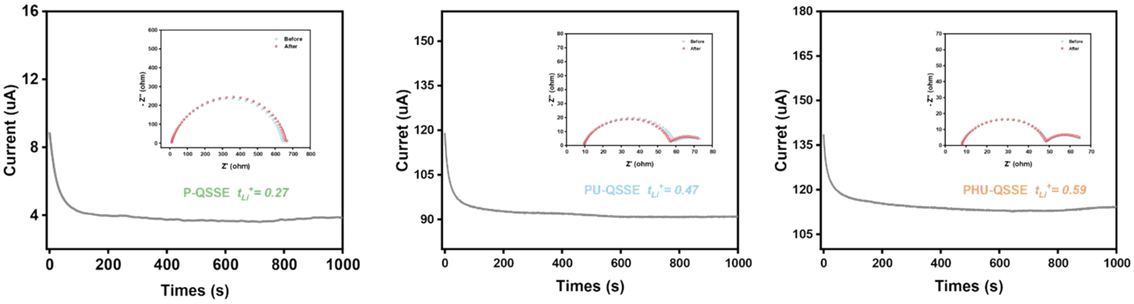

Fig. S16 Li^{+} transfer number of different QSSEs.

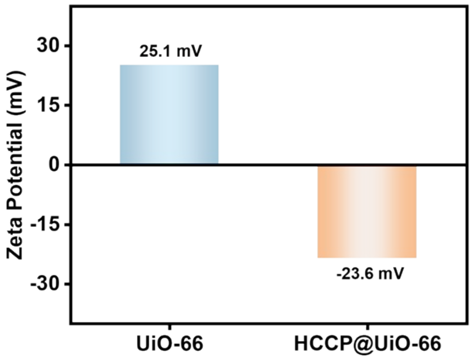

Fig. S17 The Zeta potential of UiO-66 and HCCP@UiO-66.

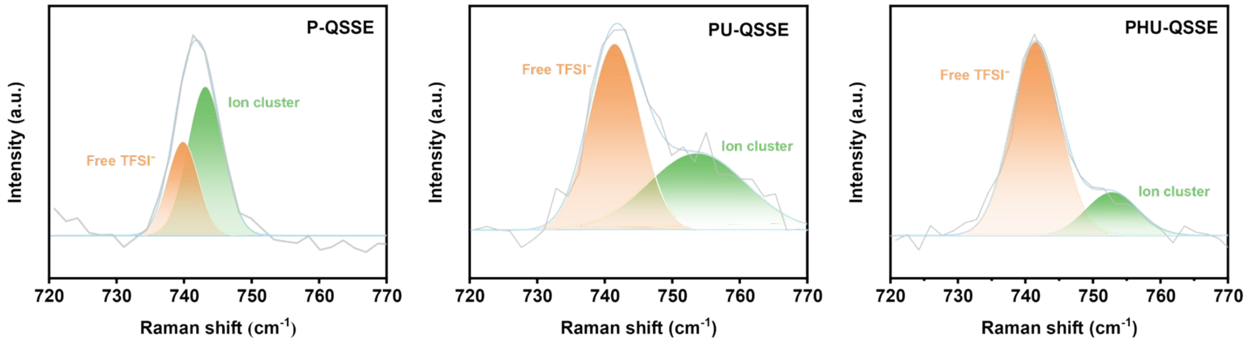

Fig. S18 Raman spectra of QSSEs mainly at 730–755 cm^{-1}.

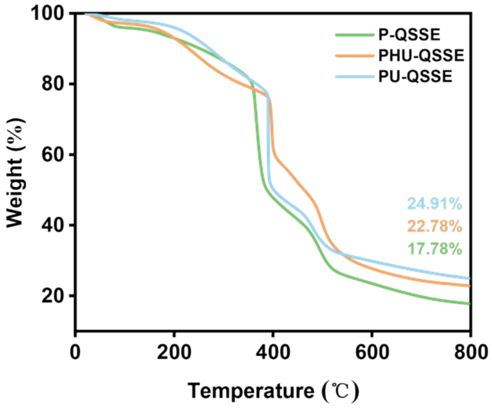

Fig. S19 TGA of different QSSEs.

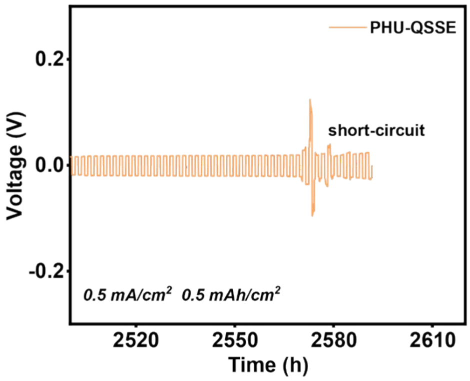

Fig. S20 Short-circuit of the Li|PHU-QSSE|Li battery at 2520 - 2580 h.

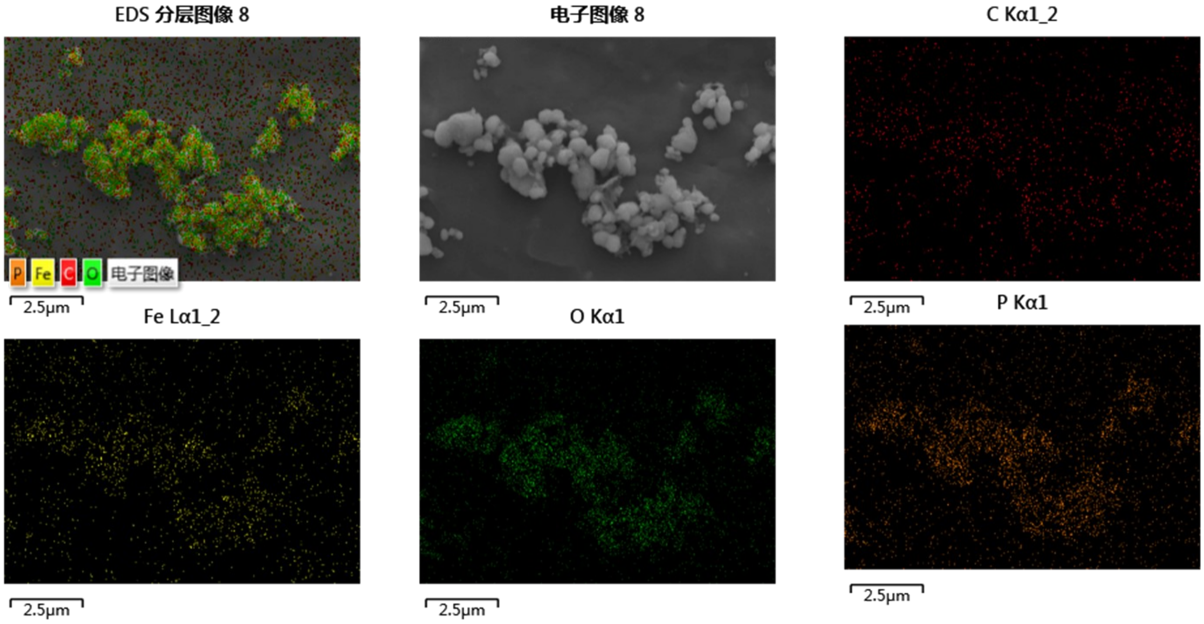

Fig. S21 The SEM image of the LFP and the EDS mapping of elementals C, Fe, O and P.

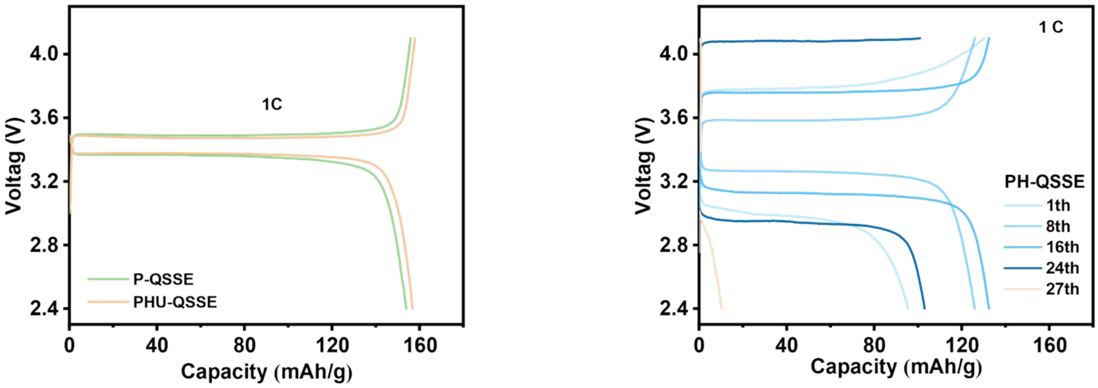

Fig. S22 Discharge-charge curves of battery with P-QSSE and PH-QSSE at 1C

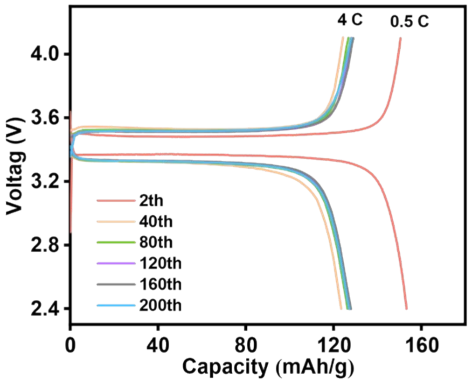

Fig. S23 Discharge-charge curves of the Li|PHU-QSSE|LFP battery at 4 C.

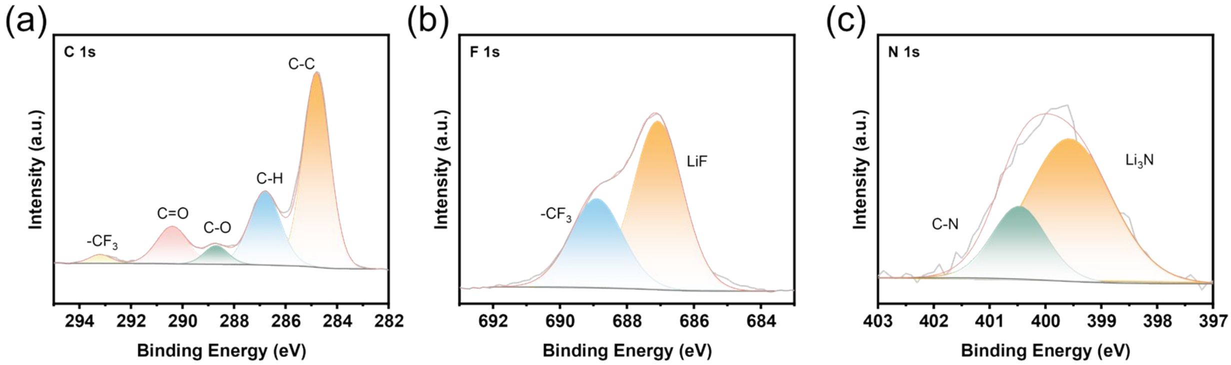

Fig. S24 (a,b,c) XPS spectra of cycled lithium metal surface of LFP|PHU-QSSE|Li cell after 5 cycles, showing C 1s, F 1s and N 1s spectra.

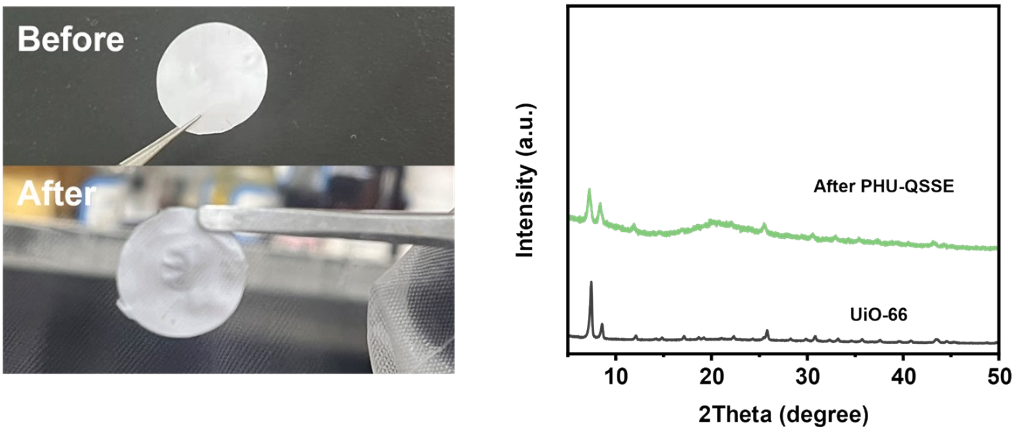

Fig. S25 Optical photos and XRD pattern of PHU-QSSE after the LFP||Li cell cycling.

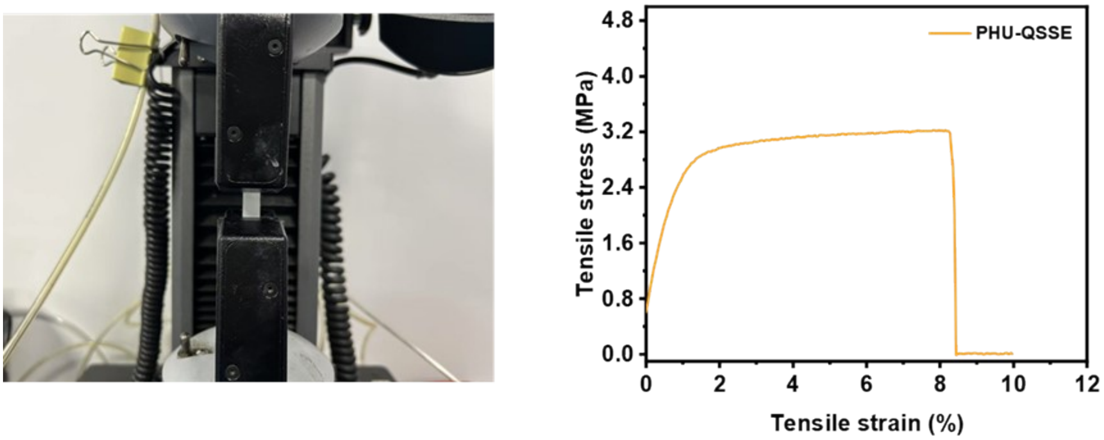

Fig. S26 Optical photos and stress-strain curves of mechanical properties test of PHU-QSSE.